

Journal of Biomedical Optics

SPIEDigitalLibrary.org/jbo

***In vivo* low-coherence spectroscopic measurements of local hemoglobin absorption spectra in human skin**

Nienke Bosschaart
Dirk J. Faber
Ton G. van Leeuwen
Maurice C. G. Aalders



In vivo low-coherence spectroscopic measurements of local hemoglobin absorption spectra in human skin

Nienke Bosschaart,^a Dirk J. Faber,^{a,b} Ton G. van Leeuwen,^{a,c} and Maurice C. G. Aalders^a

^aUniversity of Amsterdam, Academic Medical Center, Department of Biomedical Engineering and Physics, P.O. Box 22700, NL-1100 DE Amsterdam, The Netherlands

^bUniversity of Amsterdam, Academic Medical Center, Department of Ophthalmology, P.O. Box 22700, NL-1100 DE Amsterdam, The Netherlands

^cUniversity of Twente, Biomedical Photonic Imaging Group, P.O. Box 217, NL-7500 AE Enschede, The Netherlands

Abstract. Localized spectroscopic measurements of optical properties are invaluable for diagnostic applications that involve layered tissue structures, but conventional spectroscopic techniques lack exact control over the size and depth of the probed tissue volume. We show that low-coherence spectroscopy (LCS) overcomes these limitations by measuring local attenuation and absorption coefficient spectra in layered phantoms. In addition, we demonstrate the first *in vivo* LCS measurements of the human epidermis and dermis only. From the measured absorption in two distinct regions of the dermal microcirculation, we determine total hemoglobin concentration (3.0 ± 0.5 g/l and 7.8 ± 1.2 g/l) and oxygen saturation. © 2011 Society of Photo-Optical Instrumentation Engineers (SPIE). [DOI: 10.1117/1.3644497]

Keywords: spectroscopy; low-coherence; absorption; attenuation; hemoglobin; human skin.

Paper 11408LR received Jul. 28, 2011; revised manuscript received Sep. 8, 2011; accepted for publication Sep. 9, 2011; published online Oct. 14, 2011.

The derivation of physiological parameters from the spectroscopic determination of tissue optical properties can offer a fast and painless alternative to invasive diagnostic procedures such as tissue biopsies and drawing of blood. For instance, the absorption coefficient of the dermal microcirculation is directly related to the tissue hemoglobin concentration, which provides information on oxygen saturation, blood volume, and potentially the hemoglobin concentration in whole blood. A variety of spectroscopic techniques is available for measuring tissue optical properties.^{1,2} However, these techniques have limited ability to confine their probing volume to embedded structures such as the dermal microcirculation (located beneath the epidermis), or require long photon path lengths (several mm to cm) which exceed the adult dermal thickness ($\pm 0.2 - 1.2$ mm).³ Consequently, many of those techniques rely on assumption-based algorithms

to account for layered media.⁴ Low-coherence interferometry techniques, such as low-coherence spectroscopy^{5,6} (LCS) and spectroscopic optical coherence tomography^{7,8} (SOCT) do not suffer from this limitation, since they control the size and position of the probed volume from which the optical properties are determined (lateral and in depth)—i.e., they reject the detection of photons that originate from outside the volume of interest.

We recently validated LCS on homogeneous phantoms with controlled optical properties, to quantitatively obtain the attenuation μ_t , absorption⁵ μ_a , scattering μ_s , and backscattering⁶ μ_b coefficients between 480 and 700 nm [bold-faced characters denote wavelength (λ) dependent parameters]. In this study we present, for the first time to our knowledge, quantitative measurements of local μ_t and μ_a spectra within selected volumes of inhomogeneous turbid media. We validate our method by retrieving the dye concentration from the measured μ_a of an Intralipid-dye phantom ($\mu_s = 4$ to 6 mm⁻¹, $\mu_a = 0$ to 5 mm⁻¹), covered by light attenuating layers with varying optical densities (0.39 to 0.89). Subsequently, we demonstrate the first *in vivo* LCS measurements of μ_t and μ_a of the human epidermis and dermal microcirculation, from which we determine total hemoglobin concentrations and oxygen saturation.

To obtain μ_t and μ_a from a target volume, we measured backscattered power spectra $S(\ell)$ at controlled geometrical path lengths ℓ of the light in the medium (path length and depth related parameters are corrected for the refractive index n of the medium). Our LCS system, which is described in detail in Ref. 5, is optimized for the wavelength range of 480 to 700 nm. We controlled ℓ by translating the reference mirror in steps of 27 μ m. By translating the sample in the axial direction, focus tracking of the spot size ($\phi = 5$ μ m) in the medium is achieved. Around ℓ , the signal is modulated by scanning the piezo-driven reference mirror (23 Hz), resulting in a scanning window of $\Delta\ell \approx 44$ μ m in the medium. The optical power at the sample is 6 mW.

A multimode fiber ($\phi = 62.5$ μ m) guides the reflected light from both arms to a photodiode. Fourier transformation of the acquired time signal results in spectra $S(\ell)$ with spectral resolution $\Delta\lambda = \lambda^2/(n\Delta\ell)$ (4 nm $<$ $\Delta\lambda$ $<$ 9 nm).⁵ To minimize the influence of speckle noise on $S(\ell)$, we spatially average 90 to 250 spectra by translating the sample and measuring $S(\ell)$ every 5 μ m. Fitting the single exponential decay model $S(\ell) = A \cdot \exp(-\mu_t \cdot \ell)$ (free running fit parameters A and μ_t) to the background corrected $S(\ell)$ versus ℓ , results in a μ_t spectrum.⁶ Uncertainties in A and μ_t are estimated by their 95% confidence intervals (c.i.).

When $S(\ell)$ is dominated by single backscattered light, the attenuation coefficient $\mu_t = \mu_s + \mu_a$. Since the dependence of μ_s on wavelength can be described by $a \cdot \lambda^{-b}$, least-squares fitting of $\mu_t = a \cdot \lambda^{-b} + \sum_i (c_i \cdot \mu_{a,i})$ results in the individual contributions of μ_s and μ_a to the measured μ_t . The free running fit parameters a , b , and c_i are constraint to positive values. The wavelength dependent $\mu_{a,i}$ are the known absorption spectra (unit: mm⁻¹ per unit concentration) of the contributing chromophores i with contribution c_i , which are μ_a of the dye for the phantom measurements and μ_a of deoxygenized hemoglobin (Hb) and oxygenized hemoglobin (HbO₂) for the *in vivo* skin measurements.⁹ The μ_a of the dye was obtained from a

Address all correspondence to: Nienke Bosschaart, University of Amsterdam, Academic Medical Center, Biomedical Engineering and Physics, Meibergdreef 9, Amsterdam, Noord-Holland 1100DE Netherlands; Tel: 0031205665207 Fax: 0031206917233; E-mail: n.bosschaart@amc.uva.nl.

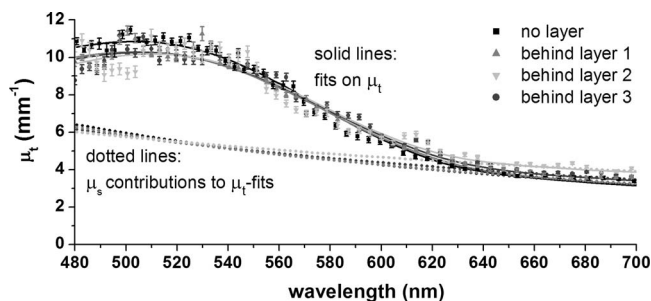


Fig. 1 Measured μ_t (dots) of a 1% Intralipid-10% dye phantom behind no layer and three TiO_2 -silicon layers (1: $D = 155 \mu\text{m}$, $\mu_t = 2.5 \text{ mm}^{-1}$; 2: $D = 170 \mu\text{m}$, $\mu_t = 5 \text{ mm}^{-1}$; 3: $D = 355 \mu\text{m}$, $\mu_t = 2.5 \text{ mm}^{-1}$). Fits on μ_t , and μ_s -contributions to the μ_t -fits are shown for all measurements.

transmission measurement.⁵ Since we are primarily interested in the total hemoglobin concentration ($[\text{tHb}] = c_{\text{HbO}_2} + c_{\text{Hb}}$) and the oxygen saturation ($\text{SO}_2 = c_{\text{HbO}_2}/[\text{tHb}]$) with their uncertainty estimates ($\pm 95\%$ c.i.) for the *in vivo* measurements, we directly fit the $[\text{tHb}]$ and the SO_2 by substituting $c_{\text{HbO}_2} = \text{SO}_2 \cdot [\text{tHb}]$ and $c_{\text{Hb}} = (1 - \text{SO}_2) \cdot [\text{tHb}]$ in the fitting algorithm.

The volume from which we obtain μ_t is controllable in both size and position inside the medium, by choosing the region for lateral averaging and the ℓ -interval for fitting the exponential decay model. When measuring on inhomogeneous media such as skin, spatial information is needed to confine our region of interest to, e.g., the epidermal or dermal layer. Therefore, we support our analysis by reconstructing an OCT image from the individual LCS time signals within every $\Delta\ell$ in the axial and lateral direction, using depth scaling $d = \ell/2$. The axial resolution of these “fused” OCT images is given by the coherence length of the light source of $\sim 1.5 \mu\text{m}$ and is therefore higher than the axial resolution of $22 \mu\text{m}$ for $S(\ell)$.

Figure 1 shows the measured μ_t (dots) of a medium consisting of 1% Intralipid (Intralipid®20%, Fresenius Kabi, Germany) and 10% magenta dye (Ecoline #337, Royal Talens, The Netherlands), uncovered and covered by nonabsorbing silicon-titanium dioxide (TiO_2) layers.¹⁰ The three covering layers varied in thickness D and scattering (layer 1: $D = 155 \mu\text{m}$, $\mu_t = 2.5 \text{ mm}^{-1}$; layer 2: $D = 170 \mu\text{m}$, $\mu_t = 5 \text{ mm}^{-1}$; layer 3: $D = 355 \mu\text{m}$, $\mu_t = 2.5 \text{ mm}^{-1}$) resulting in optical densities ($\text{OD} = D \cdot \mu_t$) of 0.39 to 0.89. The measurement volume ($1250 \times 484 \mu\text{m}^2$, width \times depth) from which we acquired μ_t was confined to the Intralipid-dye medium, directly behind the layer-medium interface. μ_t agrees within $\sim 10\%$ of the measured values, indicating that the measurement of μ_t is unaffected by the optical density of the layer covering the medium. Also, the fits on μ_t (solid lines) and the μ_s -contribution to the fits (dotted lines) are minimally affected by the covering layers. Fitted scatter powers b of the medium are 1.8 ± 0.1 , 1.8 ± 0.2 , 1.6 ± 0.2 , 1.1 ± 0.3 for the medium covered by no layer, layer 1, layer 2, and layer 3, respectively. The dye concentration was fitted with $10.2 \pm 0.5\%$, $9.3 \pm 0.7\%$, $9.2 \pm 0.9\%$, and $9.3 \pm 0.6\%$, resulting in a maximum deviation of 0.8% from the expected dye concentration of 10%.

The upper right corner of Fig. 2 shows the OCT image that was reconstructed from an *in vivo* measurement on the skin of the palmar side of a stretched finger joint that was stabilized with light pressure against a glass slide. Index-matching gel

(Euroband Pedicat, Pollak, France) was applied at the glass-tissue interface to minimize specular reflections. We selected regions in the presumed epidermis (Region 1: $715 \times 88 \mu\text{m}^2$) and dermis (Region 2: $440 \times 418 \mu\text{m}^2$, Region 3: $1080 \times 418 \mu\text{m}^2$) for obtaining μ_t . The fit on the measured μ_t of the epidermis [Fig. 2(a)] only shows the contribution of scattering ($b = 3.5 \pm 0.3$) and neglects the absorption of hemoglobin ($[\text{tHb}] = 0 \text{ g/l}$), which agrees with the expected absence of blood vessels in this skin layer.

Within the dermis, we can distinguish two regions with relatively high (Region 2) and low (Region 3) homogeneity. The measured μ_t differ considerably between the two regions [Fig. 2(b)], which can be ascribed to a difference in both scatter power ($b = 0.5 \pm 0.1$ in Region 2, $b = 2.0 \pm 0.1$ in Region 3) and absorption. The μ_a -spectra of both regions are shown in Figs. 2(c) and 2(d). The fitted $[\text{tHb}]$ of $3.0 \pm 0.5 \text{ g/l}$ in Region 2 and $7.8 \pm 1.2 \text{ g/L}$ in Region 3 indicate the presence of blood and can be related to normal dermal blood volume fractions of 2% and 5%, respectively, when assuming a fixed hemoglobin concentration of 150 g/l for whole blood.⁹ The fitted SO_2 of $81 \pm 34\%$ in Region 2 and $100 \pm 31\%$ in Region 3 are also within physiological range.

Presumably, Region 3 encloses a flexure line and Region 2 encloses surrounding skin, since relative differences in hemoglobin absorption up to 63% were found between those two palmar skin regions during stretching,³ which is consistent with our $[\text{tHb}]$ results. This also explains the difference in scattering between the two regions, because tissue homogeneity and organization of collagen fiber content, the major contributor to dermal scattering, differ significantly between these skin regions.³ The value of the μ_s -contributions to the measured μ_t fall within the physiological range¹ of 1 to 100 mm^{-1} , but the actual dermal μ_s may be underestimated due to the contribution of multiple scattering to the LCS signal.⁶ Nevertheless, since absorption takes place along the controlled photon path,⁵ this contribution does not influence the determination of μ_a .

These *in vivo* measurements show that LCS can be used to measure hemoglobin concentration and oxygenation in the microcirculation. Although no gold standard exists to confirm our *in vivo* $[\text{tHb}]$ and SO_2 determinations, their values are convincing biologically and the optical properties from which they were derived are within the range of optical properties that were validated in our phantom study. The accuracies at which we determined $[\text{tHb}]$ ($\sim 15\%$) and SO_2 ($\sim 30\%$) are influenced by the homogeneity of their distribution within the investigated region, and by the accuracy of the determination of μ_t . The latter is affected by the size of the investigated region (i.e., the number of spatial averages and the length of the ℓ -interval for fitting the exponential decay model) and the OD of the medium covering this region, which limits the maximum probing depth of LCS to ~ 0.5 to 1 mm *in vivo*. The limiting accuracy of the *in vivo* determination of $[\text{tHb}]$ can be expected to be 8%, as found for the dye concentration in the phantoms. Since the epidermal OD (~ 0.8) is comparable to the OD's of the layers in our phantom study, the extra inaccuracy of the $[\text{tHb}]$ and SO_2 determination can be ascribed to the skin's heterogeneity.³ Although the size of the investigated region improves accuracy, it negatively affects measurement speed. Faster acquisition can be achieved by optimizing this trade-off, and by investigating the possibility for Fourier domain acquisition. In contrast to time domain

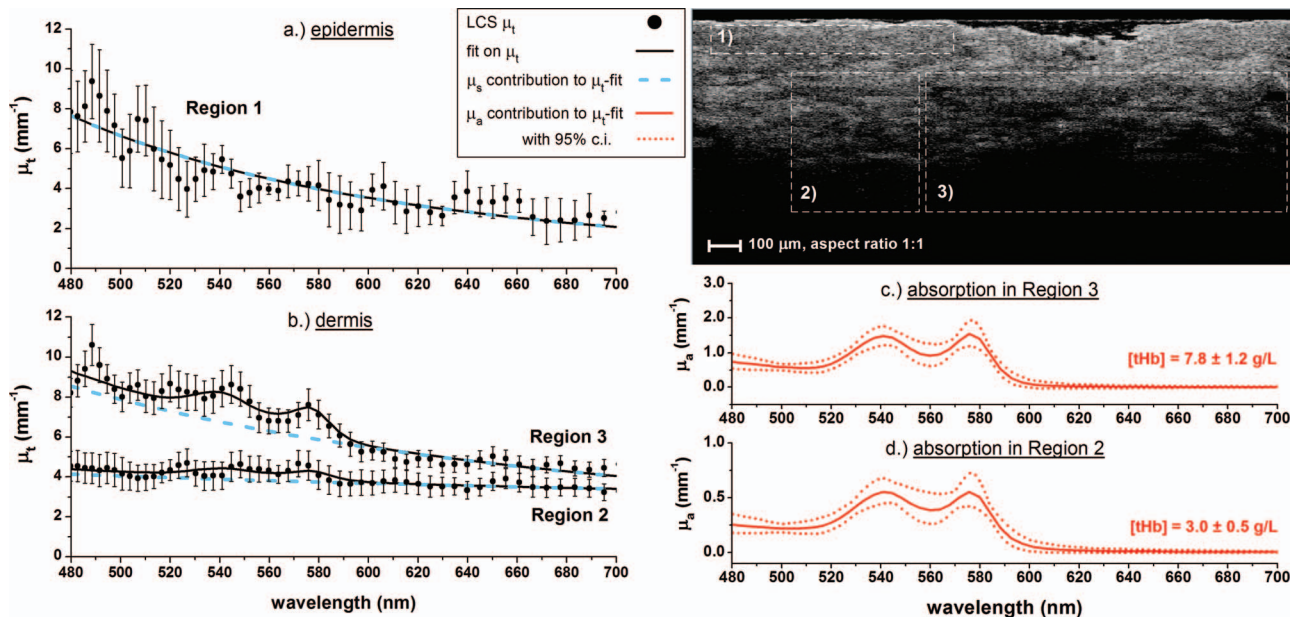


Fig. 2 *In vivo* measurement on the skin of the palmar side of a finger joint. The measured μ_t , fits on μ_t and μ_s -contributions to the μ_t -fits are shown in (a) for the epidermis (Region 1) and (b) for the dermis (Regions 2 and 3). The μ_a -contributions to the μ_t -fits are shown in (c) for Region 3 and (d) Region 2 (note the difference in vertical axis scaling). The selected regions are shown in the OCT image in the upper right corner.

acquisition, the latter will require correction for unwanted signal attenuation due to out-of-focus detection and sensitivity roll-off in depth.^{8,12}

Potentially, the dermal [tHb] can be related to the hemoglobin concentration in whole blood, if the blood volume within the investigated region can be assessed. A possible method that deserves further investigation for this purpose is obtaining the blood volume from the OCT image by assessing the vessel density using advanced signal analysis, for instance as described in Ref. 11. When measuring other tissue types, the contribution of additional chromophores (e.g., bilirubin, melanin) to the measured μ_t may need to be incorporated in our analysis. Also, a correction for Doppler broadening or shifting of the measured μ_t spectra may be needed for tissues that exhibit blood flow. We did not observe any of those influences on the measured μ_t spectra in Fig. 2(b), which can be explained by a temporary decrease of blood flow due to applied pressure on the skin.

In conclusion, we have shown that we can use LCS to locally obtain absorption coefficient spectra within confined volumes of optically inhomogeneous media. This enabled us to perform the first *in vivo* LCS measurements of hemoglobin concentration and oxygen saturation inside the dermal microcirculation. By confining the measurement volume to specific tissue structures, LCS overcomes the limitations of conventional spectroscopic techniques. LCS therefore offers a potential alternative to invasive drawing of blood for the determination of whole blood hemoglobin concentration and oxygen saturation.

Acknowledgments

This research is funded by personal grants in the Vernieuwingsimpuls program (DJF: AGT07544; MCGA: AGT07547) by the Netherlands Organization of Scientific Research (NWO) and the Technology Foundation STW.

References

1. R. Richards-Kortum and E. Sevick-Muraca, "Quantitative optical spectroscopy for tissue diagnosis," *Ann. Rev. Phys. Chem.* **47**, 555–606 (1996).
2. R. L. P. van Veen, A. Amelink, M. Menke-Puymers, C. van der Pol, and H. J. C. M. Sterenborg, "Optical biopsy of breast tissue using differential path-length spectroscopy," *Phys. Med. Biol.* **50**, 2573–2581 (2005).
3. T. C. Wright, E. Green, J. B. Phillips, O. Kostyuk, and R. A. Brown, "Characterization of a 'blanch-blush' mechano-response in palmar skin," *J. Invest. Dermatol.* **126**, 220–226 (2006).
4. A. Kienle, M. S. Patterson, N. Dognitz, R. Bays, G. Wagnieres, and H. van den Bergh, "Noninvasive determination of the optical properties of two-layered turbid media," *Appl. Opt.* **37**(4), 779–791 (1998).
5. N. Bosschaart, M. C. G. Aalders, D. J. Faber, J. J. A. Weda, M. J. C. van Gemert, and T. G. van Leeuwen, "Quantitative measurements of absorption spectra in scattering media by low-coherence spectroscopy," *Opt. Lett.* **34**, 3746–3748 (2009).
6. N. Bosschaart, D. J. Faber, T. G. van Leeuwen, and M. C. G. Aalders, "Measurements of wavelength dependent scattering and backscattering coefficients by low-coherence spectroscopy," *J. Biomed. Opt.* **16**, 030503 (2011).
7. D. J. Faber, E. G. Mik, M. C. G. Aalders, and T. G. van Leeuwen, "Toward assessment of blood oxygen saturation by spectroscopic optical coherence tomography," *Opt. Lett.* **30**, 1015–1017 (2005).
8. F. E. Robles, S. Chowdhury, and A. Wax, "Assessing hemoglobin concentration using spectroscopic optical coherence tomography for feasibility of tissue diagnostics," *Biomed. Opt. Express* **1**, 310–317 (2010).
9. Data tabulated from various sources compiled by S. Prahl, <http://omlc.ogi.edu/spectra>.
10. D. M. de Bruin, R. H. Bremmer, V. M. Kodach, R. de Kinkelder, J. van Marle, T. G. van Leeuwen, and D. J. Faber, "Optical phantoms of varying geometry based on thin building blocks with controlled optical properties," *J. Biomed. Opt.* **15**, 025001 (2010).
11. L. An, J. Qin, and R. K. Wang, "Ultrahigh sensitive optical microangiography for *in vivo* imaging of microcirculations within human skin tissue beds," *Opt. Express* **18**, 8220–8228 (2010).
12. F. Robles, R. N. Graf, and A. Wax, "Dual window method for processing spectroscopic optical coherence tomography signals with simultaneously high spectral and temporal resolution," *Opt. Express* **17**, 6799–6812 (2009).